P. TODOROVIĆ, B. JEREMIĆ, I. MAČUŽIĆ,
A. BRKOVIĆ, U. PROSO

RESEARCH

Vibration Analysis of Cracked Rotor During Run-Up

Tendency of development and use of contemporary rotor based machines is moving towards increase in revolution speed, increase of load with simultaneous reduction in dimensions and mass. These contradictory demands as a result offer significantly unfavourable rotor tension levels, which makes them vulnerable to appearance of the fatigue induced cracks. Development of fatigue cracks can have extremely damaging effects on reliability of rotating machinery with huge rotating masses. Analysis of dynamical behaviour of rotor with cracks is a topic which preoccupied huge attention of great number of authors in the last four decades of twentieth century.
Results of experimental vibration analysis during the run-up period have been given in this paper. Results of RMS velocity of vibrations, harmonic components 1×, 2×, 3× and 4×, as well as diagrams of displacement and phase angle has been presented. By analyzing the results of experimental research shown in this paper, conclusion can be made that the change of second harmonic (2×) component resembles a parameter which can be earliest indicator of crack appearance.

Keywords: vibration analysis, rotor, crack detection, run-up

1. INTRODUCTION

Reliable identification of rotor crack is quite vital in order to prevent the fault, which can cause high damage. Research done so far proved that by tracking the total vibration level you can determine the existence of the crack only in final phase, which, in the most cases, is unacceptable.

Detailed review of over 350 studies which consider the effect of crack development on dynamical rotor behaviour was given by *Dimarogonas* [1]. He concluded that the crack is represented by new harmonics in the spectre of vibrations. Apart from appearance of the second harmonic (2×) of rotation, as well as the subharmonic of critical speed, according to *Dimarogonas*, it's necessary to be aware to two families of harmonics, which can appear as a consequence of crack development, as follows:

1. Higher harmonics of the rotation speed due to nonlinearity of the closing crack, and
2. Longitudinal and torsion harmonics are present in the start-up lateral vibration spectrum due to the coupling.

Crack also leads to reduction in rotor natural frequencies, [1, 4, 9] because with the crack development a reduction in rotor rigidness occurs. Apart from this, with development of fatigue crack, beside the change in rotor natural frequencies, there is a significant increase in oscillation amplitude during the critical speed zones [4, 9].

Sekhar (2003) [7] presents an analysis by which he deducts that it's easier to detect the existence of the crack by analysis of dynamical behaviour of rotor during run up or coast-down rather then by analysis of its behaviour during stationary operation mode.

2. TRANSVERSAL CRACK DEVELOPMENT MODELS

Widely applied model of transversal fatigue crack development is the breathing crack model [1, 7, 8, 9]. One of the simplest breathing crack model of rotor with transversal crack is shown in Figure 1.

Petar Todorović[1)], Branislav Jeremić[1)],
Ivan Mačužić[1)] Aleksandar Brković[1)], Uroš Proso[1)]
[1)] Faculty of Mechanical Engineering,
Sestre Janjić 6, 34000 Kragujevac, Serbia

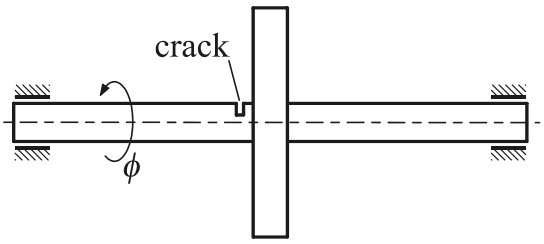

Figure 1. Rotor model with crack [7]

When there is existence of a crack on the rotor, during the rotor rotations there is closing and opening of the crack, which causes the time varying rigidness of the rotor. In order to predict dynamical behaviour of rotor with breathing crack method more precisely, it's fundamental for a mathematical model which describes the crack to be as precise as possible. In Figure 2 there are two simple models that represent the function of the crack opening and closing $f(t)$.

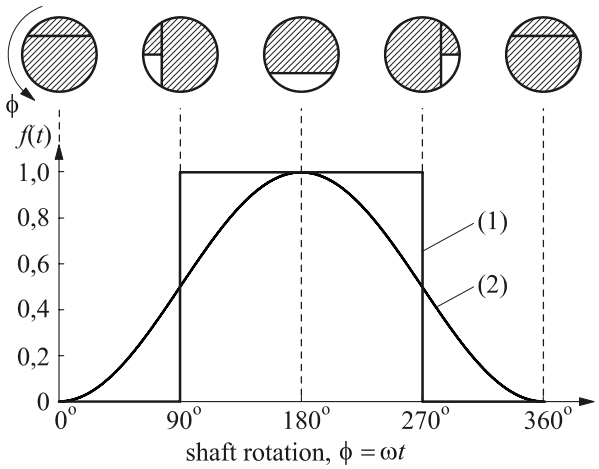

Figure 2. Crack models [7, 8, 9]

According to the model (1) in Figure 2, the opening/closing function of the crack $f(t)$ can have values 1 (open) or 2 (closed) as follows:

$$f(t)=\begin{cases}0 \quad za \quad \phi\in\left(-\dfrac{\pi}{2},\dfrac{\pi}{2}\right)\\ 1 \quad za \quad \phi\in\left(\dfrac{\pi}{2},\dfrac{3\pi}{2}\right)\end{cases} \qquad (1)$$

In case when the gravity force is significantly greater then the force of unbalance, the crack model (2) according to Figure 2 is recommended, that can be represented as:

$$f(t)=\frac{1}{2}(1-\cos\omega t) \qquad (2)$$

In this paper, a *non-dimension crack depth* α [8, 9, 11] is adopted for measuring the crack development level, and it represents the ratio of crack depth a and shaft diameter d (Figure 3):

$$\alpha=\frac{a}{d} \qquad (3)$$

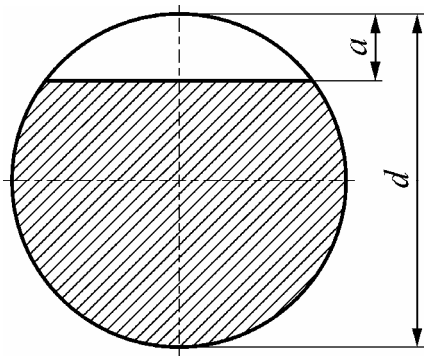

Figure 3. Common crack parameters

3. FREQUENCY ANALYSIS OF NON STATIONARY SIGNALS

As it's already mentioned, in this study, the effect of fatigue crack on oscillatory behaviour of rotor has been analyzed, during rotor's run-up period. Vibration signal during the run-up period of the rotor is non-stationary by its nature. Traditional frequency analysis application (FFT algorithm) to the non-stationary signals leads to dissipation of the harmonic components which are dependable on rotor's rotating speed.

In order to overcome the pre-mentioned limitation, during the process of discretization we use the external synchronization signal which affects the frequency of discretization. Vibrations signal is in that case shown by same number of discrete values for each rotor revolution. This way it's provided that the frequency of discretization is synchronized with the revolution speed of the rotating machine, and this is called the *synchronous sampling.* The most important advantages of synchronized discretization are shown in reference [6]. The usage of *synchronous sampling* is often implemented in the modern measurement system and vibration analysis.

Synchronous sampling can be obtained, when, after discretization of the synchronization signal and signal of the vibrations with constant frequency of discretization, the technique of resampling and interpolation [2] is applied, what is shown in Figure 4. Synchronization signal $s(t)$ is gained by key phasor which generates one impulse per rotor revolution.

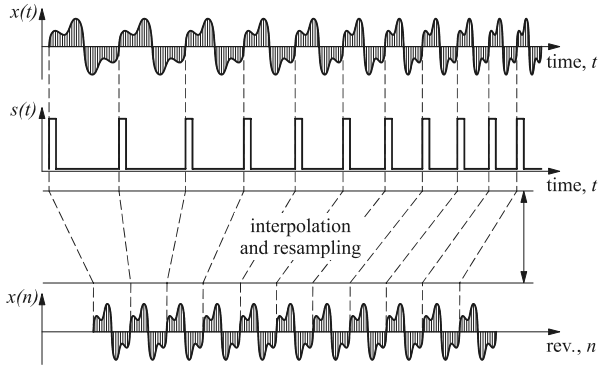

Figure 4. Interpolation and resampling technique [2]

- $x(t)$, vibration signal as the function of time,
- $s(t)$, synchronization signal as the function of time, and
- $x(n)$, vibration signal as the function of revolutions

If Fourier's transformation is applied after *synchronous sampling* the *order spectrum* is obtained [2, 3]. This technique is used during experimental research described in this paper.

4. EXPERIMENT METHODOLOGY

For experimental investigations of the effect of rotor crack development on its oscillatory behaviour, the test equipment shown in Figure 5 is used [10].

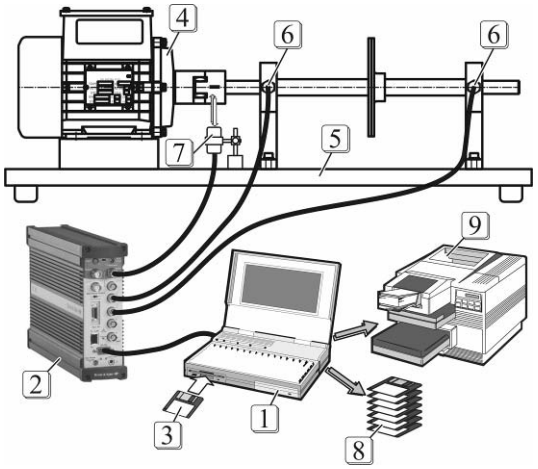

Figure 5. Test equipment [10]

Test equipment consists of the rotational machine model (position 5 in Figure 5) which is driven by a 3-phase asynchronous motor (position 4 in Figure 5). Motor is connected to an inverter, which allows the run-up parameters to be defined.

In order to monitor the dynamic behaviour of rotor, two piezoelectric accelerometers are used, (position 6 in Figure 5). For the purpose of synchronous sampling laser key phasor is used (position 7 in Figure 5) which generates one impulse per rotor revolution. The PULSE platform type 3560-B (position 2 in Figure 5) and data recorder software (position 3 in Figure 5) which is installed on a notebook computer (position 1 in Figure 5) are used for discretization of the signal from above mentioned transducers. Measurement results (position 8 in Figure 5) can be archived, further processed, or printed (position 9 in Figure 5).

Schematically model of the investigated rotor and the position of the transversal crack during the experimental research are shown in the Figure 6. The diameter of the shaft on the place where crack is simulated is $d = 20mm$ (Figure 3). Measurement points where vibration transducers M1 and M2 were positioned are shown in Figure 6. Measurement direction was horizontal.

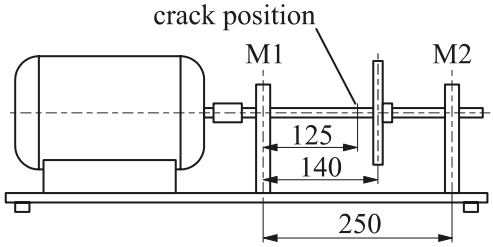

Figure 6. Schematic model [10]

Run-up duration was $20s$, acquisition time was approximately $22s$ and the frequency of discretization was $10kHz$. Appropriate anti-aliasing filter was used as well. Level of unbalance which was added to the rotor disc with diameter of $150mm$ is $m_u = 2g$. Investigated crack depths are shown in Table 1.

Table 1. Crack depths for which research has been done

Crack depth *a, mm*	Non-dimension crack depth α, -
0	0
2	0,100
4	0,200
6	0,300
8	0,400
10	0,500
11	0,550
12	0,600
13	0,650
14	0,700
15	0,750
16	0,800
17	0,850
18	0,900
18,5	0,925
18,8	0,940
19	0,950

Shaft appearance before and after the experiment is shown in Figure 7.

Figure 7. Shaft a) before and b) after experiment

Typical vibration signal waveform in time domain, measured on the measuring points M1 and M2 has been shown in Figure 8. Shorter segment of the signal from key phasor and vibration transducers has been shown in Figure 9.

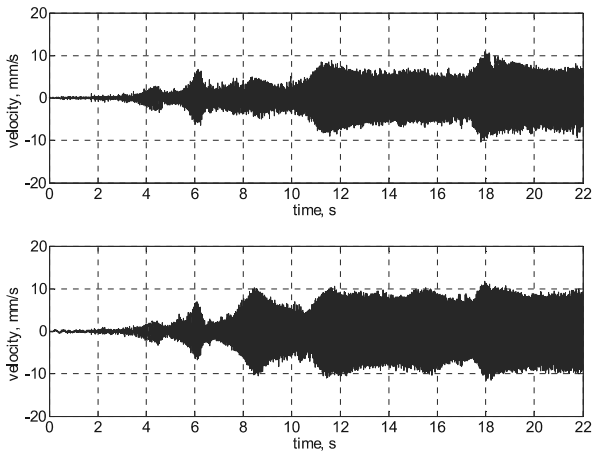

Figure 8. Signal waveform in time domain

Diagram of revolution speed change during run-up indicates that the change is nearly linear in time (Figure 10). From this diagram it can be noticed that the maximum revolution speed (RPM) was $n_{\max} \approx 4750\,\mathrm{min}^{-1}$ or $f_{\max} \approx 79Hz$.

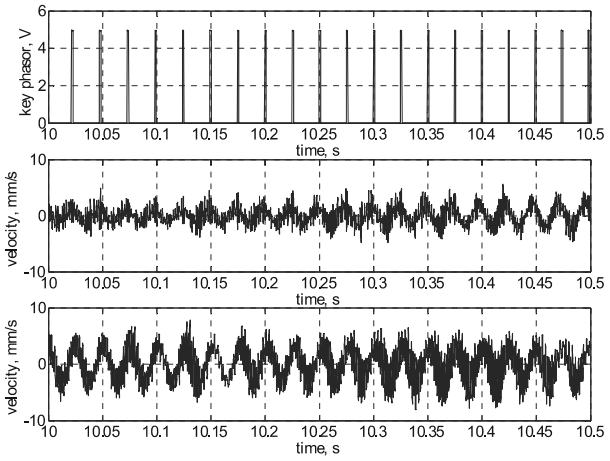

Figure 9. Segment of signal waveform

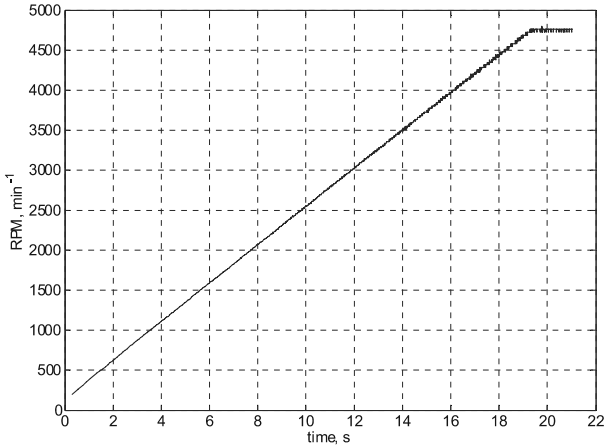

Figure 10. Revolution speed change during run-up period

By analyzing the vibration signals in the time domain during the run-up period the existence of resonant phenomenon can be noticed, though it is hard to determine for which revolution speed they occur.

As the vibration signals are measured during the run-up period it means that the signals are non stationary ones. The synchronous sampling process of the signal shown in the Figure 8 is done by using the specially developed algorithm for digital re-sampling and interpolation which is described more in detail in the reference [10]. Further signal processing after synchronous sampling which included frequency analysis and order tracking was done in MATLAB and is also described in reference [10].

5. RESULTS AND DISCUSION

Results of experimental research have been shown by 3-d diagrams, where the change of the considered vibration parameter is given on *z*-axis as the function of the revolution speed (from $500\,\mathrm{min}^{-1}$ to $4700\,\mathrm{min}^{-1}$) (*x*-axis) and as the function of the development of crack depth α (*y*-axis). All parameters are shown for measuring points M1 and M2. Presented results are from reference [10].

Changes in the RMS velocity of vibrations are shown on diagrams in Figure 11 and Figure 12. From these diagrams it can be noticed that for $\alpha \approx 0{,}8$ there is no significant change in the vibration levels. For higher values of non-dimension crack depth there is an increase in the vibration level, and it is mostly in areas of revolution speed higher then $2500\,\mathrm{min}^{-1}$.

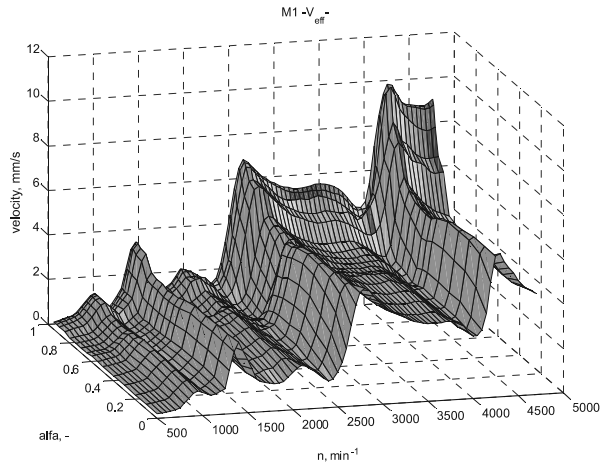

Figure 11. RMS velocity – M1

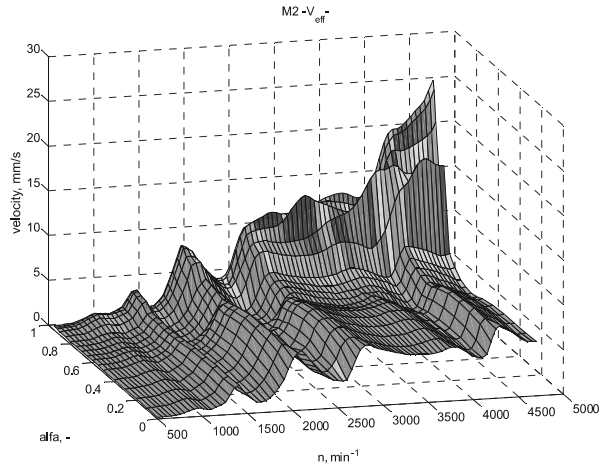

Figure 12. RMS velocity – M2

A relative change of RMS velocity has been shown in Figure 13 and Figure 14. These values represent the difference of RMS velocity for the considered non-dimension crack depth α and RMS velocity for $\alpha = 0$. Those diagrams confirms above mentioned annotation which refers to zones where the increase in the vibration level occurs (for $\alpha > 0{,}8$ and $n > 2500\,\mathrm{min}^{-1}$).

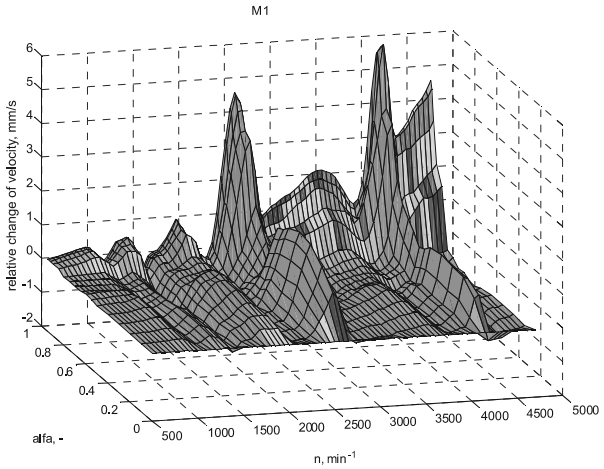

Figure 13. Relative change of RMS velocity compared to $\alpha = 0$ – M1

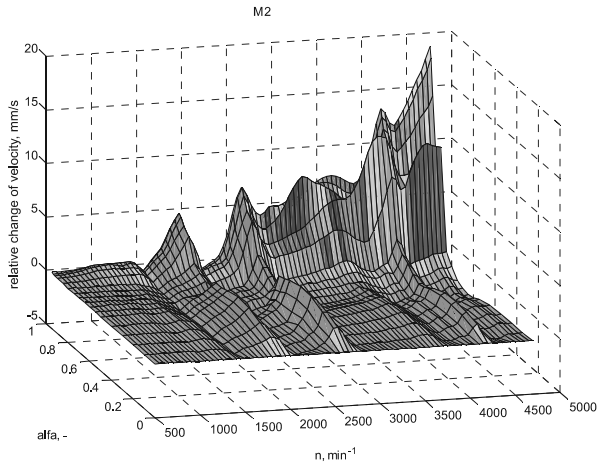

Figure 14. Relative change of RMS velocity compared to $\alpha = 0$ – M2

Changes of the first (1×), (Figure 15 and Figure 16), the second (2×) (Figure 17 and Figure 18), the third (3×) (Figure 19 and Figure 20) and the fourth (4×) (Figure 21 and Figure 22) harmonics of velocity indicate that there is a significant change of target harmonic components with increase of the non-dimension crack depth α. The change in the second (2x) harmonic (Figure 17 and Figure 18) occurs as the earliest (for $\alpha > 0{,}5$). With further increase in non-dimension crack depth the second (2×) harmonic has the highest increase (in absolute value, over $12 mm/s$ for the measuring point M2).

Diagrams of other harmonic components (1×, 3×, and 4×) also show the tendency of increase for the values of non-dimension crack depth $\alpha > 0{,}6$. As absolute value, only the change of the fourth (4×) harmonic component is significant (for the values of $\alpha > 0{,}8$).

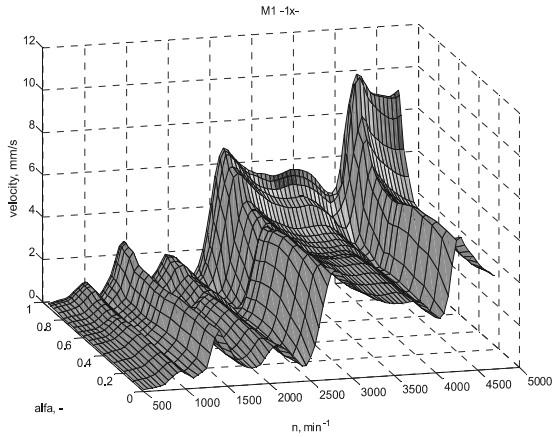

Figure 15. The first harmonic – M1

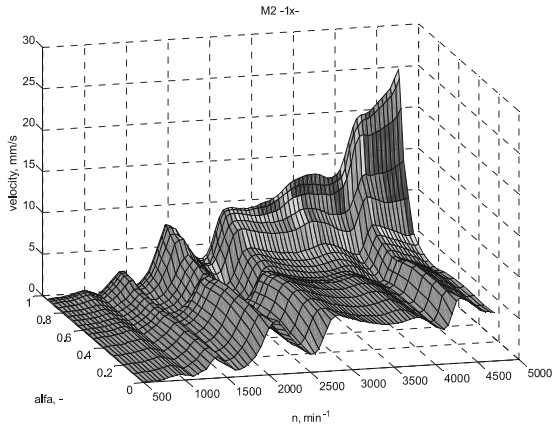

Figure 16. The first harmonic – M2

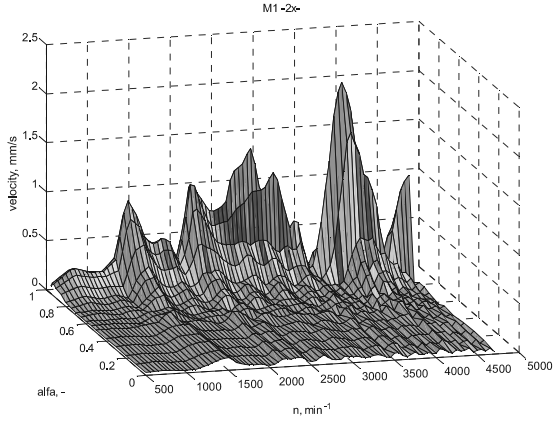

Figure 17. The second harmonic – M1

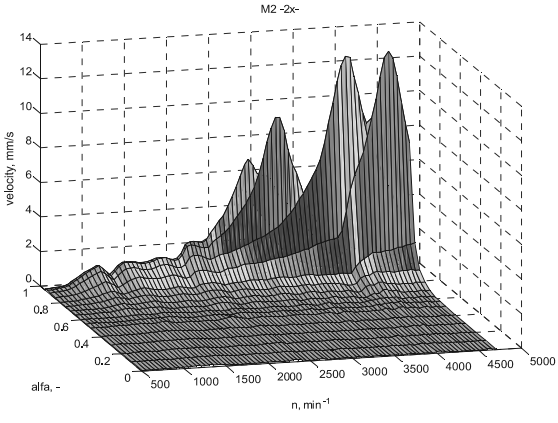

Figure 18. The second harmonic – M2

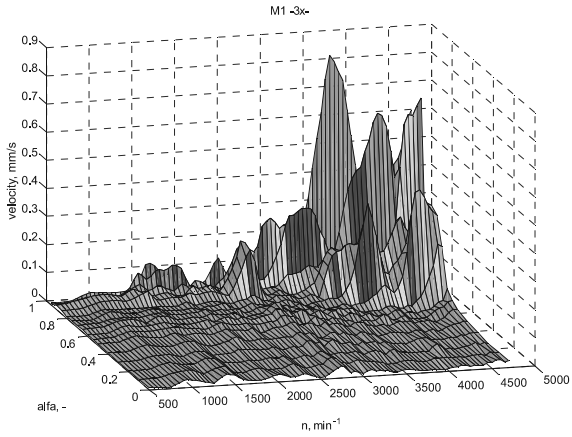

Figure 19. The third harmonic – M1

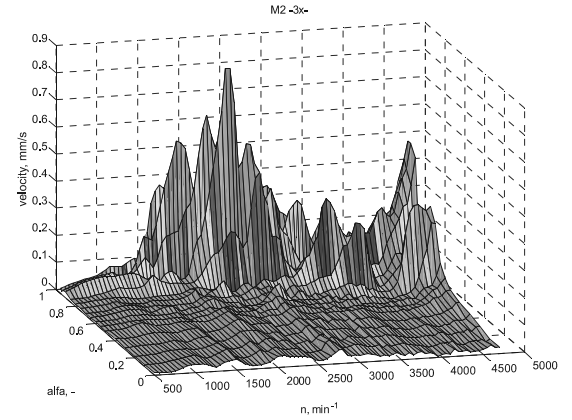

Figure 20. The third harmonic – M2

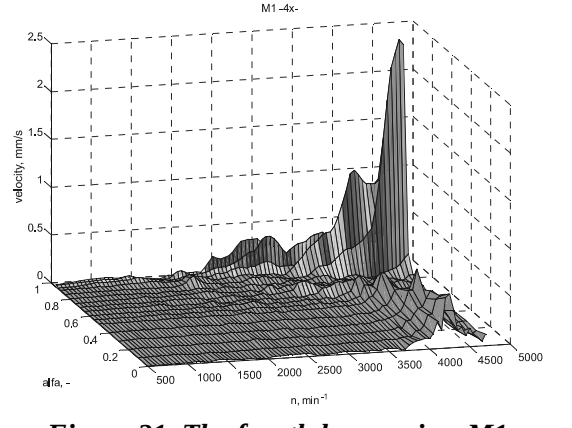

Figure 21. The fourth harmonic – M1

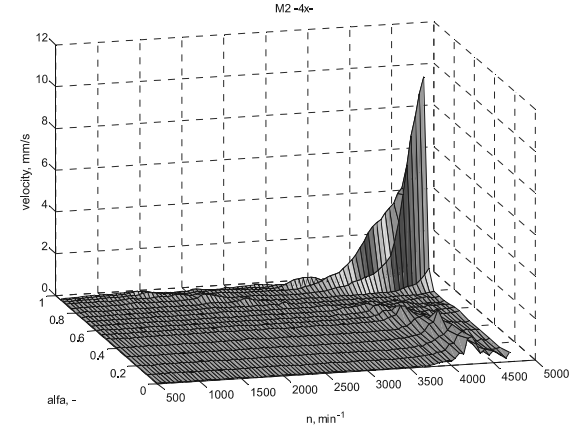

Figure 22. The fourth harmonic – M2

Diagrams of the displacement change are shown in Figure 23 and Figure 24. These diagrams are derived by numeric integration of change of the first (1×) harmonic of velocity diagrams shown in Figure 15 and Figure 16. For numerical integration, the following equation has been used:

$$x = \frac{v}{\omega} = \frac{v}{2 \cdot \pi \cdot f} = \frac{30 \cdot v}{\pi \cdot n} \qquad (4)$$

where: x is displacement, v is velocity, ω is circular frequency, f rotational frequency and n revolution speed. And $f = \frac{n}{60}$. Displacement change tendency is identical as tendency of effective values of velocity change (Figure 11 and Figure 12), and the tendency of change in the first (1×) harmonic component (Figure 15 and Figure 16).

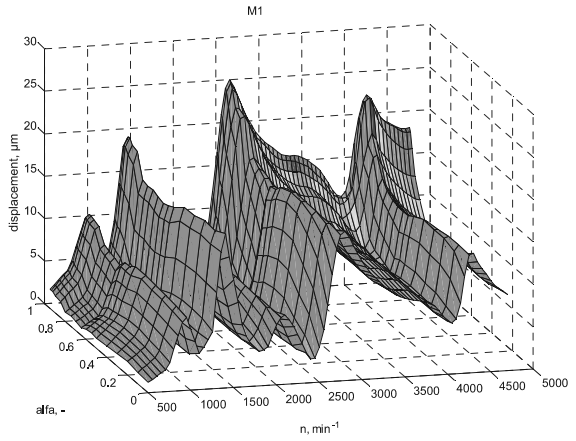

Figure 23. Displacement – M1

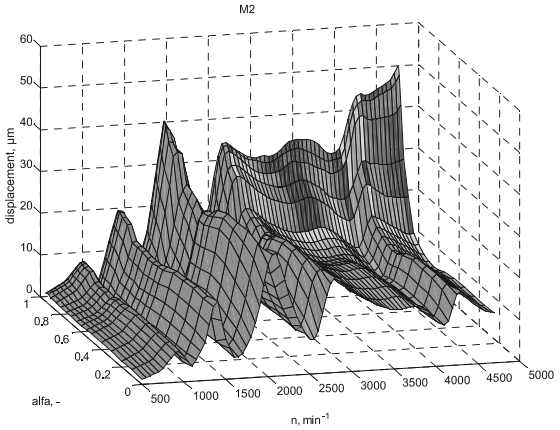

Figure 24. Displacement – M2

The phase angle change is shown on Figure 25 and Figure 26. It is hard to notice from these diagrams if there is a change of the phase angle with the change of the crack depth. In order to accomplish easier analysis, diagrams of relative change of phase angle have been introduced (Figure 27 and Figure 28). These diagrams represent the difference of phase angle for the considered non-dimension crack depth α and phase angle for $\alpha = 0$.

From diagrams of relative change of phase angles it can be concluded that the most intensive change of phase angles is in critical speed zones. It can be concluded that there is translation of critical speed zones, that is, change of its natural frequency.

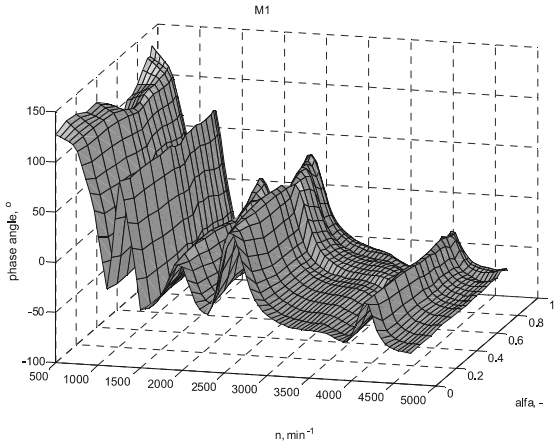

Figure 25. Phase angle – M1

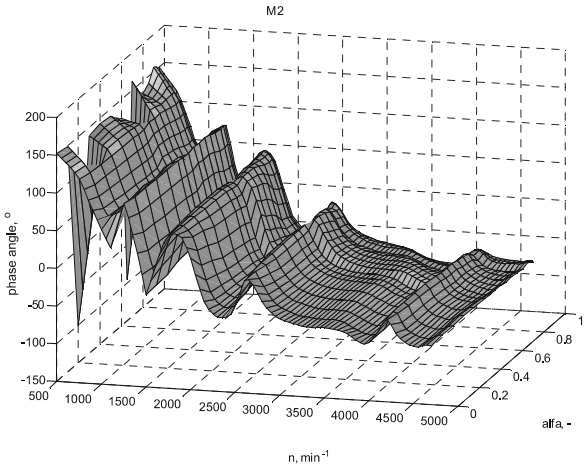

Figure 26. Phase angle – M2

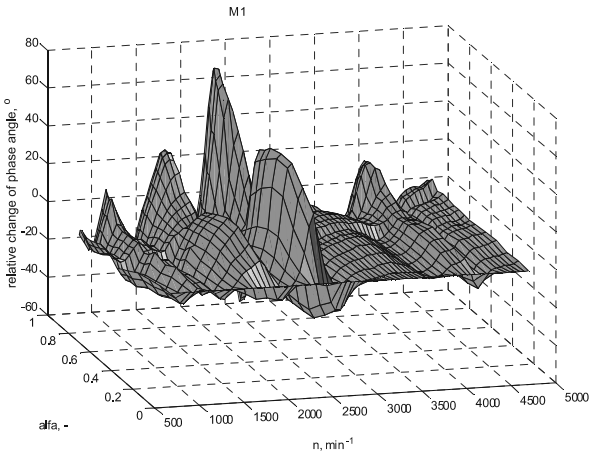

Figure 27. Relative change of phase angle compared to $\alpha = 0$ – M1

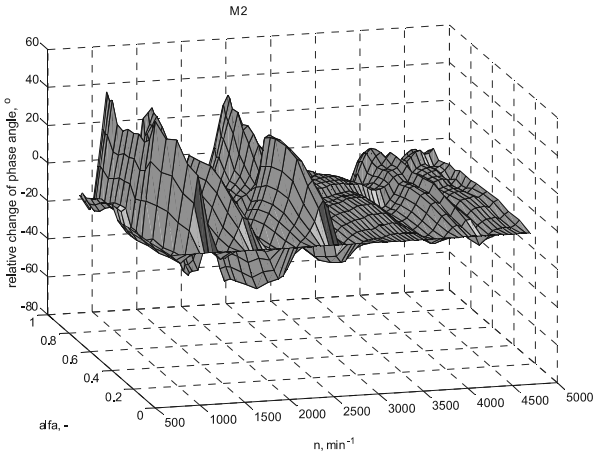

Figure 28. Relative change of phase angle compared to $\alpha = 0$ – M2

6. CONCLUSION

After the analysis of shown results, it can be concluded that by development of rotor crack, a significant changes of parameters which describe the oscillatory behaviour of rotor during the run-up period has been noticed. Of all chosen parameters, diagram showing changes of the second (2×) harmonic is the earliest indicator of crack appearance for the observed rotor. With crack development, there is relocation of critical speed zones, which is pointed on diagrams of phase angle changes. Results of experimental studies have shown that methodology presented in this paper can be used for identification of rotor crack development.

REFERENCES

[1] Dimarogonas D. A. (1996) Vibration of cracked structures: A state of the art review, *Engineering Fracture Mechanics*, Vol. 55, No. 5, 1996., pp. 831-857

[2] Gade S., Herlufsen H., Konstantin-Hansen H., Wismer N. (1995) Order Tracking Analysis, *Brüel&Kjær Technical Review*, No.2, 1995

[3] Gade S., Herlufsen H., Konstantin-Hansen H., Vold H. (1999) Characteristics of the Vold-Kalman Order Tracking Filter, *Brüel&Kjær Technical Review* No.1, 1999

[4] Green I., Casey C. (2005) Crack detection in a rotor dynamic system by vibration monitoring – Part I: Analysis, *Journal of Engineering for Gas Turbines and Power*, ASME, Vol. 127, April 2005., pp. 425-436

[5] Darpe A. K. (2007) A novel way to detect transverse surface crack in a rotating shaft, *Journal of Sound and Vibration* 305 (2007), pp. 151-171

[6] ISO 13373-2:2005(E) (2005) Condition monitoring and diagnostics of machines – Vibration condition monitoring–, Part II: Processing, analysis and presentation of vibration, *International Organization for Standardization*

[7] Sekhar A. S. (2003) Crack detection through wavelet transform for a run-up rotor, *Journal of Sound and Vibration* (2003) 259 (2), pp. 461-472

[8] Sekhar A. S. (2004) Crack identification in a rotor system: a model-based approach, *Journal of Sound and Vibration* 270 (2004), pp. 887-902

[9] Sinou J-J., Lees A.W. (2005) The influence of cracks in rotating shafts, *Journal of Sound and Vibration* 285 (2005), pp. 1015-1037

[10] Todorović P. (2006) Kompleksna dijagnostika rotora, Doctor of Philosophy Thesis, *Mašinski fakultet u Kragujevcu*, 2006

[11] Wu M.-C., Huang S.-C. (1998) Vibration and crack detection of a rotor with speed dependent bearing, *International Journal of Mechanical Sciences*, Vol. 40, No 6 (1998), pp. 545-555